Analytical and Experimental Comparison of Heavy Vehicle Loads on Pavements

KANG-MING HSU, DONALD A. STREIT, AND BOHDAN T. KULAKOWSKI

A vehicle's vertical dynamic wheel force acting at the tire-road interface is a significant factor in causing pavement damage. Work that involved configuring a two-axle, 66,750-N (15,000-lbf) truck for dynamic wheel force measurement is described. Strain gauges were installed in a shear strain measurement mode on the axle housing of the vehicle. Inertia compensation was included when calculating tire-road forces. A 12.7-mm (0.5-in.) step and a 2-Hz sinusoid with a 12.7-mm (0.5-in.) peak-to-peak amplitude were used as inputs to a hydraulic vehicle shaker. The measured vehicle response data were in good agreement with those predicted by computer simulation.

Theoretically, a vehicle traveling on a perfectly smooth, straight, horizontal road at a constant speed will apply constant forces to the road through its tires, its static wheel loads (neglecting out-of-balance forces generated by the vehicle itself). In practice this condition never actually occurs because all roads have surface irregularities that excite the vehicle suspension system and cause a fluctuating force component on the road. This force, superimposed on the static wheel load, is frequently called the dynamic wheel force or the dynamic tire force (*1*). Knowledge of the magnitude of dynamic wheel forces is important for a variety of reasons:

1. Damage to a road structure is related to the magnitude of applied wheel forces.
2. Vibrational behaviors of highway bridges are determined by dynamic wheel forces.
3. Dynamic wheel forces applied to the road generate ground vibrations that can be an annoyance and that can cause damage to adjacent buildings.
4. A vehicle's road-holding ability is affected by the magnitude of the dynamic variations of wheel force; for instance, if the variations are large enough for a wheel to lose contact with the road surface, the vehicle's braking ability will be impaired.
5. The magnitude of the dynamic variation of wheel force is related to the forces applied to the vehicle body and hence to the ride quality of the vehicle.

These concerns, among others, are the motivating factors for the development of methods for dynamic wheel force measurement.

The force at the tire-road interface can be determined either in the pavement or on the vehicle. To continuously monitor this force directly it would be necessary to mount a continuous force-sensing instrument to the surface of a tire. Because this is not yet possible, many indirect or discrete measuring systems have been devised. Sensors have been mounted both in pavements and on trucks. Although vehicle-mounted systems do not provide direct wheel-pavement force measurement, they offer continuous force data. Vehicle-mounted systems are usually used on a long-term, continuous basis for studying the loads developed by vehicles traveling over various pavement types. One advantage of these methods is that a single instrumented vehicle can be used on numerous roads, allowing study of various surface conditions and pavement types. One disadvantage is that each vehicle in a study must be instrumented. Only vehicle-mounted systems that are generally used to measure dynamic wheel forces are considered in this paper. Typical vehicle-mounted systems are described first. Implementation of an experimental system is then described, and results from experiments and simulations are compared.

Pennsylvania Transportation Institute, The Pennsylvania State University, 201 Research Office Building, University Park, Pa. 16802.

BACKGROUND

Tire pressure as a means of monitoring wheel-pavement forces has been discussed in works by Fisher and Huckins (*2*) and Whittemore et al. (*3*). A differential tire pressure transducer is used to measure the change in tire pressure as wheel forces are applied to a tire. Transducer response can reflect wheel force. The differential pressure-load relationship is affected by tire pressure and tire volume. However, Whittemore et al. (*3*) found that the precision of this method is not acceptable because of nonlinear and phase-shift relationships between pressure change and wheel force.

Tire deflection has been related to wheel-pavement load measurement by Magnusson (*4*), Dickerson and Mace (*5*), and Hopkins and Boswell (*6*). Considering a tire as a spring, tire deflection-versus-tire load characteristics can be determined via calibration procedures. Tire deflection can then be used to calculate the wheel-pavement force. Usually, noncontact displacement transducers such as laser transducers or optical sensors are used to measure tire deflection. The load-versus-deflection relationship is usually very sensitive to tire pressure and temperature. If tire pressure or temperature changes, then such changes must be accommodated in the calculation of pavement loads.

Whittemore et al. (*3*) and others (*7,8*) have discussed the wheel force transducer method for measuring dynamic wheel-pavement loads. This system is similar to the strain-gauged axle housing system, but instead of using strain gauges a specially designed wheel force transducer is used. Different types of wheel force transducers have been developed. Usually, the wheel force transducer is designed to provide an output that is proportional to wheel loads. The advantage of this system is that it can be installed directly onto the wheels, serving as a portable measuring system available for use on many vehicles.

The strain-gauged axle housing method has been discussed by various investigators (*3,9–11*). In this method strain gauges are ce-

mented to the axle housing of a vehicle. Vertical accelerations of the axle are measured by two accelerometers installed on the vehicle axle. By adding the inertial force of the mass that is outboard of the strain gauges to the shear force sensed by the strain gauges, the force applied at the tire-road interface can be determined.

STRAIN-GAUGED AXLE HOUSING

The experimental method used in the present study is the strain-gauged axle housing method. A short summary of the instrumentation procedure is followed by descriptions of calibration procedures and wheel-pavement load calculations.

INSTRUMENTATION

Strain Gauges

The front and rear axles of a truck were instrumented. Strain gauges were cemented to the centers of two vertical surfaces of the axle housing, as close to the wheels as possible, as shown in Figure 1. In previous studies strain gauges were sometimes cemented to the top or bottom surface of the axle housing to measure normal strains due to bending. The benefit of those arrangements is that strain gauges are very sensitive to the wheel force because the maximum bending stresses occur at the top and bottom of the housing. However, if straight and steady driving is not maintained, lateral wheel forces can significantly affect strain gauge output, causing distortion of vertical wheel force measurements. In the present study strain gauges were attached to the centers of the vertical surfaces of the axle housing. They measure housing maximum shear stress and largely eliminate the effects of lateral wheel forces on vertical wheel-pavement load measurements. Strain gauge calibration showed that the shear strain gauge arrangement is sufficiently sensitive to experimentally determine vertical wheel loads on pavement.

Accelerometers

On each side of the front axle a bracket was mounted near the wheel to accommodate accelerometer mounting. On the rear axle accelerometers were mounted directly on the top centers of the leaf springs as shown in Figure 1. All accelerometers were mounted upright to measure vertical accelerations. Additionally, a thermally insulated accelerometer was installed on the right side of the rear axle adjacent to the regular accelerometer to monitor the effects of temperature on accelerometer output.

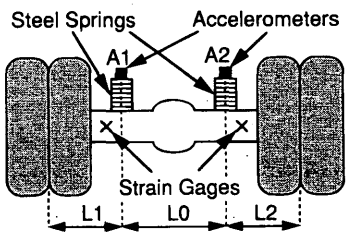

FIGURE 1 Instrumentation of rear axle.

STATIC CALIBRATION

Static strain gauge calibration was performed by progressively jacking the truck to adjust wheel load and strain gauge outputs. Wheel force was measured via a wheel scale under the tire. Five and one-half tons of dead weight were placed on the truck to increase the calibration range. Because of the difficulty of increasing the load on the front axle, the front calibration range was only from 0 to 15 570 N (3,500 lbf) on each side of the axle. The rear axle load range was from 0 to 44 480 N (10,000 lbf). Calibration results exhibited linear relationships between strain gauge output and vertical wheel force. Strain gauge calibration curves are given in Figure 2.

WHEEL-PAVEMENT LOAD FORMULATION

Tire-road forces include three components, as shown in Figure 3. In Figure 3 F_x is the traction force due to tire rolling resistance, F_y is the lateral force, which is very small and negligible compared with the other forces in the condition of straight driving, and F_z is the vertical wheel force, which causes pavement damage and affects the vibrational behavior of vehicle and road structure. F_z was the force component of interest in the present study.

The strain-gauged axle housing method requires that a strain gauge be installed at a particular section of the axle between wheel and suspension leaves. Sensor output depends on the forces transmitted from the tire-road interface to the sensor. Therefore, it is necessary to know the effects of each force on the instrumented section. During straight driving, which is typical of highway driving, lateral force is negligible. Both traction and vertical wheel force are the primary forces affecting force sensor output. Vertical wheel force

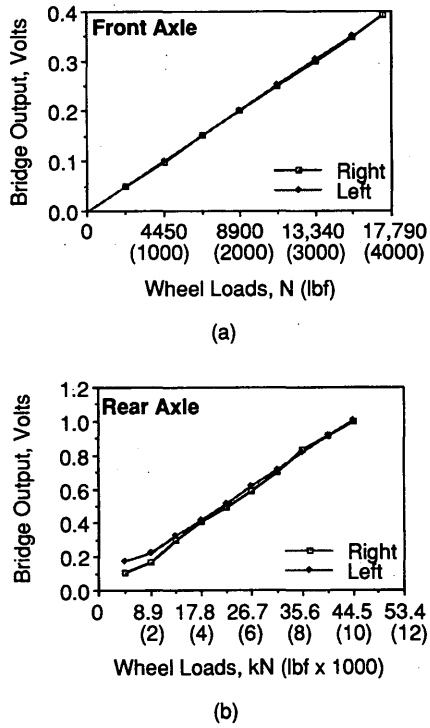

FIGURE 2 Bridge characteristics: (*a*) front axle; (*b*) rear axle.

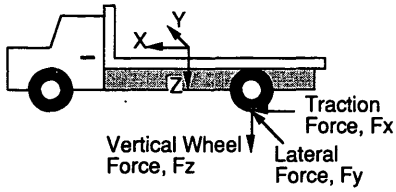

FIGURE 3 Wheel forces diagram.

causes shear and bending at the section where the sensor is installed. In addition to the shear and bending, the traction force also causes torsion. The sensing circuits used in this project were designed so that the effects of bending and torsion are largely eliminated. Therefore, the vertical shear force at the instrumented section can be determined from the strain gauge output.

In most wheel force measurement approaches, the measurement transducer is located some distance away from the point at which the force of interest is located. This is due to the difficulties involved in installing the transducer at the tire-road interface (except in instrumented pavement measuring systems). When dynamic loads vary only slowly, static calibration of the measurement system might be sufficient to determine the force applied at the tire-road interface. However, when changes of loading occur over very short time intervals, the data measured by sensors such as strain gauges or wheel force transducers are distorted by dynamic effects. Some fraction of applied force is required to accelerate the mass of the intervening structure between the point of force application and the force sensors. Adding the inertial force component of the outboard mass to that determined at the gauge location, the dynamic wheel force applied at the tire-road interface can be obtained (*12–14*). Thus, the total vertical dynamic wheel force, defined as F_z, can be expressed as

$$F_z = F_{sg} + M_{ob}A_{ob} \tag{1}$$

where

F_{sg} = force measured by strain gauges;
M_{ob} = outboard mass, which is the mass of the intervening structure between the transducer and the point of force application in this project, M_{ob} is the mass outboard of the locations of the strain gauges; and
A_{ob} = vertical acceleration of the outboard mass.

Outboard mass depends on the location of the transducer and is sometimes difficult to determine accurately. For instance, in the case of a strain-gauged axle, the outboard mass includes the tire assembly, the brake unit (drum, shoes, booster, etc.), and a part of the axle. Accurate determination of the center of the outboard mass is also important. However, the irregular shape and inhomogeneity of the outboard structure make it difficult to measure the location of the center of mass accurately. Usually, the center of mass is estimated to be at the center of the wheel or at some proximal offset. The acceleration of the center of the outboard mass is difficult to instrument directly because of axle and wheel rotation. It is therefore necessary to determine acceleration of the outboard mass geometrically with accelerometers mounted to the axle. As shown in Figure 4 the vertical acceleration of the right-hand outboard mass, A_{ob}, is calculated as

$$A_{ob} = (1 + L_2/L_0)A_2 - (L_2/L_0)A_1 \tag{2}$$

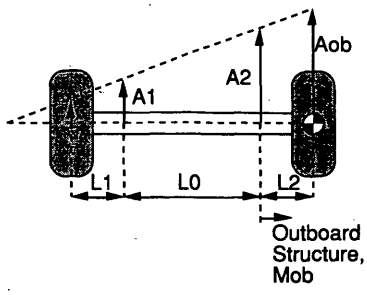

FIGURE 4 Geometric determination of acceleration.

where

A_1 = vertical acceleration measured by Accelerometer A1 in Figure 4,
A_2 = vertical acceleration measured by Accelerometer A2 in Figure 4,
L_0 = horizontal distance between two accelerometers in Figure 4,
L_2 = horizontal distance between the center of mass of the right outboard mass and Accelerometer A2, and
L_1 = horizontal distance between center of mass of the left outboard mass and Accelerometer A1.

The vertical acceleration of the left-hand side can be calculated similarly by switching the parameters A_1 and A_2 and replacing L_2 by L_1 in Equation 2.

In dynamic force measurement the closer the force sensor is to the point of force application the less the intervening structure affects the force measurement. Measurement accuracy can be increased as the effects of inertia and local bending of any nonrigid body are reduced. Also, locating the force sensor near the point of force application will minimize the unavoidable errors in the estimation of the mass and the center of mass of the intervening structure.

ADVANTAGES AND DISADVANTAGES

A major advantage of the strain-gauged axle housing method for determining dynamic wheel loads is cost. Hardware requirements for strain gauge implementation are minimal, and once it is instrumented a vehicle can be used to study many test conditions. The disadvantages of this method include the requirement of multiple strain gauges and accelerometer installation and calibration on each vehicle of interest. In addition, depending on vehicle geometry, some axles may be particularly cumbersome for strain gauge installation. Also, errors in inertial force measurement are introduced by inaccuracies in determination of the mass or the center of mass of the outboard structure, on both, and by acceleration calculation errors resulting from axle bending.

ANALYSIS OF TEST DATA

To evaluate system performance the truck was placed on a hydraulic shaker (DYNTRAC, the FHWA Dynamic Truck Actuator System), which was used to generate elevation irregularities. Two tests, a 12.7-mm (0.5-in.) step input and a 2-Hz sinusoidal input of

12.7 mm (0.5 in.) of peak-to-peak amplitude, were performed. All tests were in phase for all wheels. The sampling rate for both tests was 200 Hz. The measured data were compared with the simulation results by using the Phase 4 computer package (*15*). In the case of step input the actual DYNTRAC actuator displacement data were recorded and were used as input for simulation. For sinusoidal input the actual actuator response data were not available, and therefore, a perfect sinusoidal input was used in computer simulation. Time traces of the shear forces determined at strain gauge locations, total dynamic wheel forces, and simulation results are displayed in Plots *a*, *b*, and *c*, respectively, of Figures 5 through 8.

COMPARISON OF DYNAMIC WHEEL FORCES

To investigate the effect of wheel-axle inertia on the experimental results, Plots a and b of Figures 5 through 8 were compared. The difference between shear force (Plots *a*) at the strain gauge locations and the total dynamic wheel force (Plots *b*) is the inertial force that accelerates the outboard structure. The points labeled 1 through 10 in these plots have been identified for purposes of comparison. Equation 3 compares inertial loads (numerator in this equation) to the dynamic component of total wheel load (denominator in this equation). Values given by Equation 3 are listed in Table 1.

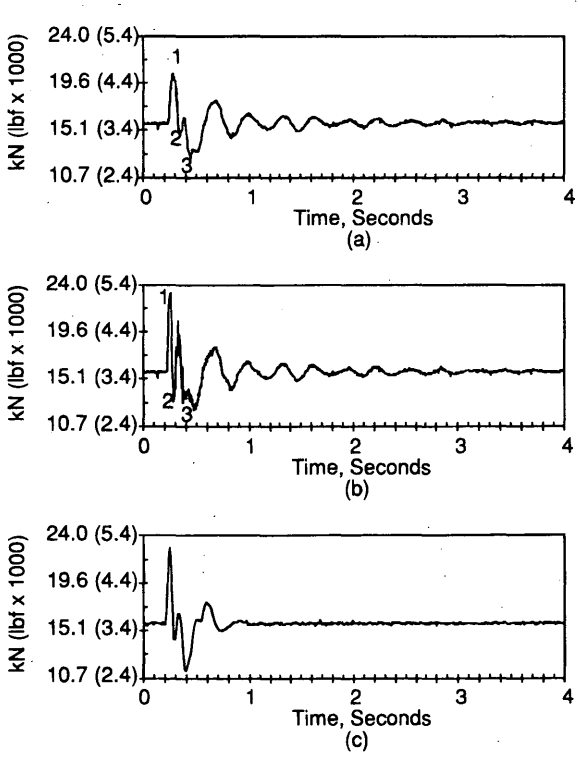

FIGURE 5 Vertical forces on front axle [127-mm (0.5-in.) step input]: (*a*) force at location of axle strain gauge; (*b*) experimental dynamic wheel force after inertial corrections according to Equation 1; (*c*) dynamic wheel force from simulation results.

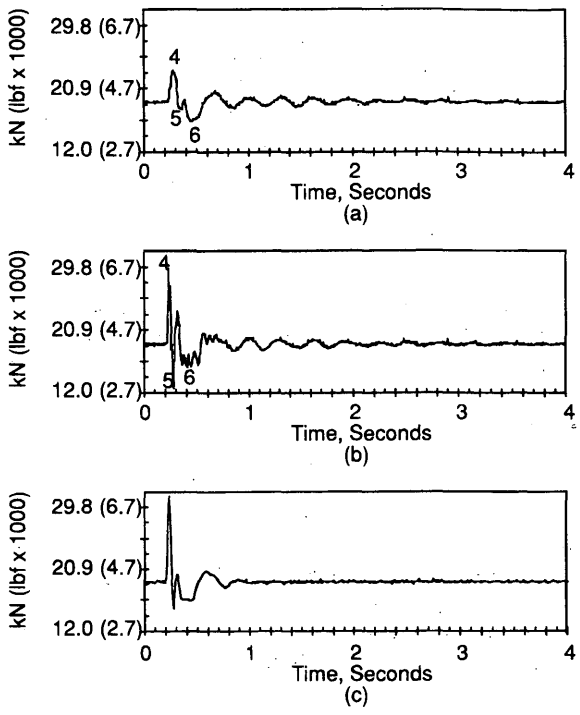

FIGURE 6 Vertical forces on rear axle [127-mm (0.5-in.) step input]: (*a*) force at location of axle strain gauge; (*b*) experimental dynamic wheel force after inertial corrections according to Equation 1; (*c*) dynamic wheel force from simulation results.

$$\text{Percent} = \left| \frac{F_i - S_i}{F_i - \overline{F}} \right| \times 100 \tag{3}$$

where

F_i = dynamic wheel force,
S_i = sensed shear force, and
$\overline{F}$ = average force.

Figures 5 to 8 and Table 1 show that in the case of sinusoidal input the inertial force is small, approximately 6 to 15 percent, because of the low excitation frequency and amplitude. Increasing the frequency or the amplitude, or both, of the excitation will largely increase this inertia effect. In the case of step input large axle acceleration resulted in a large inertial force component. For some points in step input the magnitude of this inertial force component was up to 57 to 84 percent of the amplitude of dynamic wheel force, exceeding the component of force sensed by strain gauges. The need to introduce the compensation for an inertia effect is clearly demonstrated.

When the measured dynamic wheel force and simulation results are compared, they show good agreement in shape, and the difference of magnitudes is within acceptable limits. Based on the simulation it is likely that the difference in the magnitudes in force peaks was mainly caused by the difference between the actual tire stiffnesses and those used in the simulation. In the case of step input, in addition to a resonance of about 2.5 to 3 Hz shown in the measured dynamic wheel force, a second vibration mode clearly appeared in both the measured force and the simulation result. Theoretically, both the tire stiffness and the suspension spring rate largely affect the magnitude of dynamic wheel force and its fluctuation behavior. Simulation results showed much quicker settling. Both viscous

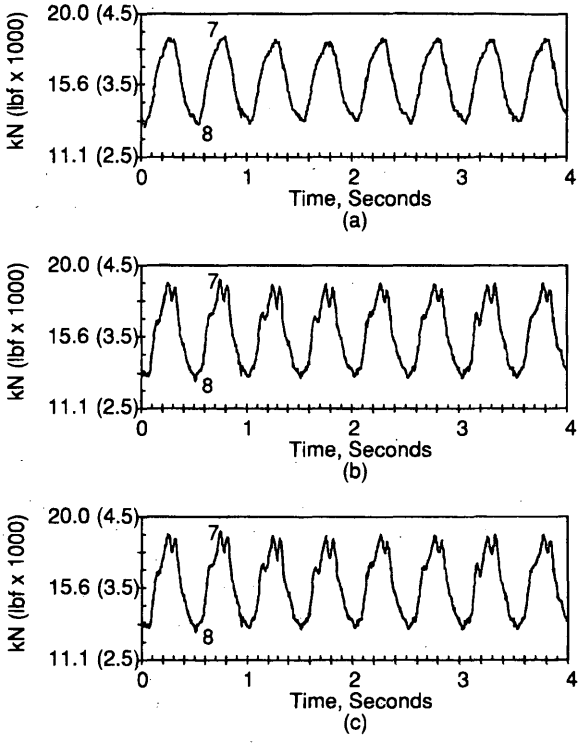

FIGURE 7 Vertical forces on front axle [sinusoidal input, 2 Hz, 63.5 mm (0.25 in.) of amplitude]: (*a*) force at location of axle strain gauge; (*b*) experimental dynamic wheel force after inertial corrections according to Equation 1; (*c*) dynamic wheel force from simulation results.

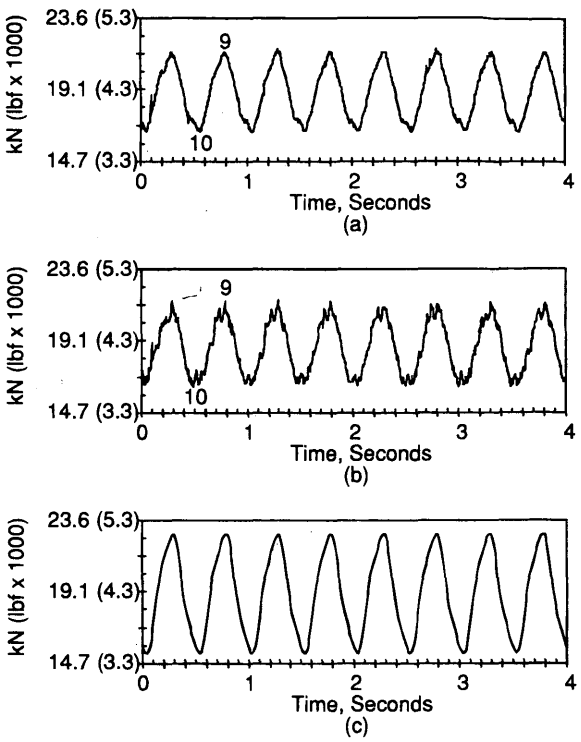

FIGURE 8 Vertical forces on rear axle [Sinusoidal Input, 2 Hz, 63.5-mm (0.25-in.) amplitude]: (*a*) force at location of axle strain gauge; (*b*) experimental dynamic wheel force after inertial corrections according to Equation 1; (*c*) dynamic wheel force from simulation results.

damping and coulomb friction affected the settling time. The comparison implied that these energy dissipation-related parameters might be too large in the simulation. Basically, computer simulation provides a theoretical value. Its results are a function of the parameters input into the program. However, some parameters are very difficult to measure. The differences between actual truck parameters and those used in the simulation result in inconsistencies between measured data and simulation results. However, a good correlation between the measured data and the simulation results has been demonstrated.

In addition to the truck parameters used in the simulation, many other factors may affect the difference between measured data and simulation results:

1. Inaccurate determination of the mass of the outboard structure will cause an error in the calculation of inertial force.
2. Inaccurate determination of the position of the center of mass of the outboard structure will cause an error in acceleration calculation, and thus, the inertial force will be distorted. This effect will be especially clear when the excitations to truck wheels are out of phase and of high roughness or frequency.
3. Geometric determination of acceleration is based on consideration of the axle moving as a rigid body. Local bending of any nonrigid body of the axle will cause the difference between the calculated and the actual accelerations. In high-frequency excitation the magnitude of this error will increase.
4. Temperature change may affect strain gauge characteristics. This effect is more important in field tests since the axle temperature may greatly increase because of braking.
5. The signal-to-noise ratio of shear strain gauge output is not large enough so that the output might be significantly affected by noise.
6. Accelerometers did not respond well in the low-frequency range.

TABLE 1 Percentage of Inertia Force of Amplitude of Dynamic Wheel Force

	Step Input			Sinusoidal Input		
Axle	Fig. No.	Data Pt.	% Diff.	Fig. No.	Data Pt.	% Diff.
Front	5	1	36.5	7	7	15.3
Front	5	2	67.8	7	8	9.5
Front	5	3	9.8	-	-	-
Rear	6	4	57.1	8	9	6.1
Rear	6	5	84.5	8	10	7.7
Rear	6	6	12.5	-	-	-

COMPARISON OF POWER SPECTRAL DENSITIES

Power spectral densities of measured dynamic wheel force and simulation results are shown in Figures 9 and 10 for a step input and Figures 11 and 12 for a sinusoidal input. Good agreement between experimental and simulation data is displayed. In the case of sinusoidal input the highest power spectral density peaks occur at 2 Hz, which is consistent with the excitation frequency. Because a perfect sinusoidal input was used in the computer simulation the difference in the power spectral density between measured data and simulation is more pronounced than in the case of step input, in which actual

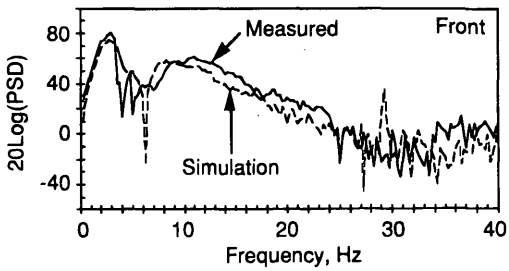

FIGURE 9 Power spectral densities of front wheel forces [127-mm (0.5-in.) step input].

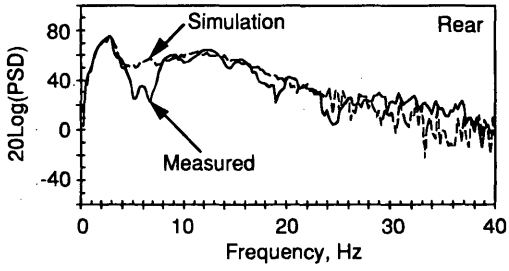

FIGURE 10 Power spectral densities of rear wheel forces [127-mm (0.5-in.) step input].

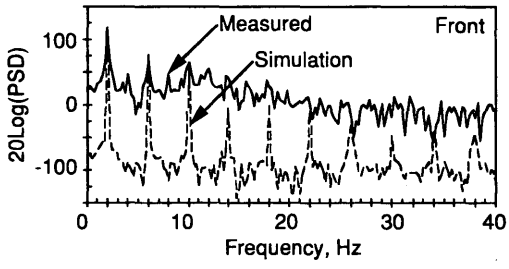

FIGURE 11 Power spectral densities of front wheel forces [sinusoidal input, 2 Hz, 63.5-mm (0.25-in.) amplitude].

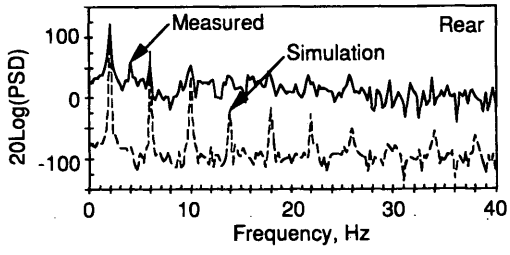

FIGURE 12 Power spectral densities of rear wheel forces [sinusoidal input, 2 Hz, 63.5-mm (0.25-in.) amplitude].

actuator output was recorded and was used as input to the computer simulation.

COMPARISON OF DYNAMIC IMPACT FACTORS

The dynamic impact factor (DIF) provides a quantitative measure of the variation of dynamic wheel forces and is defined as

$$\text{DIF} = \sqrt{\frac{\sum_{i=1}^{n} (F_i - \bar{F})^2}{(n-1)\bar{F}^2}} \tag{4}$$

where

n = number of sampled datum points,
$\bar{F}$ = average dynamic wheel force, and
F_i = dynamic wheel force at the ith datum point.

The comparison of DIFs is shown in Table 2. In the case of sinusoidal input the DIFs of the simulation results are significantly higher than those of the measured data. It is suspected that the actuator gains might be set too low, such that the amplitude of the actual actuator response was smaller than a perfect sine wave and, thus, resulted in smaller force variation. It is therefore reasonable for the measured force to have smaller DIFs. In the case of a step input, since actual actuator output was recorded for the input to the computer simulation, the DIFs of the test data and simulation results are very close.

CONCLUSIONS

Axle strain was used to determine dynamic wheel loads on pavement. Experimental data show a good correlation with analytical simulation results. Additional dynamic wheel load measurement techniques are being studied. These include dynamic wheel scales mounted on the FHWA Dynamic Truck Actuator System (DYNTRAC) and a removable wheel force transducer hub that would be mounted between a wheel and an axle. Accurate and transferable dynamic wheel force instrumentation will be used to survey the effects of vehicle parameters such as tire pressure, tire type, suspension type, and number of axles on pavement load.

During the course of the study it was of interest to know the required accuracy of the measurements of those vehicle parameters to ensure reasonable simulation results. The simulation model that has been validated experimentally as described here has been used to determine the sensitivity of dynamic wheel-pavement forces to variations in system parameters at different vehicle speeds and for different road roughness values. The results of that sensitivity analysis are reported by Lin et al.(*16*).

ACKNOWLEDGMENTS

The work reported in this paper was conducted under the sponsorship of FHWA.

TABLE 2 Comparison of DIFs

Input Function	Wheel	Test Data DIF	Simulation DIF
Step	Front	0.0626	0.0532
Step	Rear	0.0542	0.0564
Sinusoidal	Front	0.1215	0.1562
Sinusoidal	Rear	0.0871	0.1347

REFERENCES

1. Quinn, B. E., and C. C. Wilson. Can Dynamic Tire Forces Be Used as a Criterion of Pavement Condition? Highway Research Record *46*, HRB, National Research Council, Washington, D.C., 1964, pp. 88–100.
2. Fisher, J. W., and H. C. Huckins. Special Report 73: *Measuring Dynamic Vehicle Loads*. HRB, National Research Council, Washington, D.C., 1962, pp. 138–148.
3. Whittemore, A. P., J. R. Wiley, P. C. Shultz, and D. E. Pollock. *NCHRP Report 105: Dynamic Pavement Loads of Heavy Highway Vehicles*. HRB, National Research Council, Washington, D.C., 1970.
4. Magnusson, G. *Measurement of Dynamic Wheel Load*. VTI Report 279A. Swedish Road and Transport Research Institute, Linköping, Sweden, 1987.
5. Dickerson, R. S., and D. G. W. Mace. *Dynamic Pavement Force Measurements with a Two-Axle Heavy Goods Vehicle*. TRRL Supplement Report 688. Transport and Road Research Laboratory, Department of the Environment Department of Transport, Crowthorn, United Kingdom, 1981.
6. Hopkins, R. C., and H. H. Boswell. Methods for Measuring Load Transfer Through Vehicle Tires to the Road Surface. HRB Proc., Vol. 36, 1957, pp. 240–252.
7. Lysdale, C. A., and R. R. Hegmon. *Development of a Truck Wheel Force Transducer*. SAE Paper 800247. Society of Automotive Engineers, Warrendale, Pa. 1980.
8. Todd, K. B. Design Recommendations for Wheel Force Transducers. Technical Memorandum EI-TIRE-8701. Pennsylvania Transportation Institute, University Park, 1987.
9. Page, J., and J. W. Grainger. A Technique for Measuring Vehicle Dynamic Wheel Loads. *TRRL Supplement Report 98UC*, Transport Road Laboratory, Department of the Environment, Crowthorn, United Kingdom, 1974.
10. Mitchell, C. G. B., and L. Gyenes. Dynamic Pavement Loads Measured for a Variety of Truck Suspensions. Paper presented at the 2nd International Conference on Heavy Vehicle Weights and Dimensions, Kelowna, British Columbia, 1989.
11. Chi, M. C. *Analysis of Dynamic Truck-Tire Pavement Interaction*. M.S. thesis. The Pennsylvania State University, University Park, 1987.
12. Ervin, R. D., R. L. Nisonger, M. Sayers, T. D. Gillespie, and P. S. Fancher. *Influence of Truck Size and Weight Variables on the Stability and Control Properties of Heavy Trucks*. Report UMTRI-83-10/2. University of Michigan, Ann Arbor, April 1983.
13. Heath, A., and M. C. Good. Heavy Vehicle Design Parameters and Dynamic Pavement Loading. *Australian Road Research*, Vol. 15, No. 4, 1985, pp. 249–263.
14. Sayers, M., and T. D. Gillespie. Dynamic Pavement/Wheel Loading for Trucks with Tandem Suspensions. *Proc., 8th IAVSD Symposium on the Dynamics of Vehicles on Roads and on Railway Tracks*, Cambridge, Minn. 1983, pp. 517–533.
15. MacAdam, C. C., P. S. Fancher, G. T. Hu, and T. D. Gillespie. *A Computerized Dynamics of Trucks, Tractor Semi-Trailers, Doubles, and Triples Combinations: User's Manual—Phase 4*. Report UM-HSRI-80-58. Highway Safety Research Institute, Ann Arbor, Mich., 1980.
16. Lin, W.-C., Y.-C. Chen, B. T. Kulakowski, and D. A. Streit. Dynamic Wheel/Pavement Force Sensitivity to Variations in Heavy Vehicle Parameters, Speed and Road Roughness. *Heavy Vehicle Systems, International Journal of Vehicle Design*, Vol. 1, No. 2, 1994, pp. 139–155.

The findings and conclusions in this paper are those of the authors and do not necessarily represent the views of FHWA.

Publication of this paper sponsored by Committee on Strength and Deformation Characteristics of Pavement Sections.